

# Model Order Selection Techniques for the Loop Filter Design of Virtual String Instruments

Cumhur ERKUT

Helsinki University of Technology

Laboratory of Acoustics and Audio Signal Processing

Espresso, Finland

Cumhur.Erkut@hut.fi

## ABSTRACT

Finding a model that accounts for a finite set of noisy samples is a general problem in engineering. In this paper, the noisy samples are the simulated decay rates of the harmonics of a string tone, and the model has a special polynomial form. This form has been utilized as an intermediate step before designing a loop filter that can be used in model-based sound synthesis of string instruments. Analytical model selection methods have been used to obtain a reliable decay rate polynomial estimate. A method for designing the final loop filter based on the intermediate polynomial representation has been shown. The results verify the robustness of this simple method.

**Keywords:** Physical modeling, Plucked strings, Decay time, Polynomial regression, Penalization.

## 1 INTRODUCTION

Studies of damping in musical strings indicate that the exact nature of the energy losses is difficult to analyze or model accurately. [1, 2]. Different mechanisms effect the decay characteristics of the harmonics in various ways. Some of these mechanisms are only qualitatively understood. Despite this fact, there is a need for rather simple models that account for the decay characteristics in numerical simulations using finite differences [3, 4] or in model-based sound synthesis of string instruments [5, 6]. In both applications, the losses are typically simulated by inserting  $M$  odd-order time derivatives in the wave equation. Then, the frequency-dependent decay rate  $\sigma$  (inverse of the decay time  $\tau$  for 3 dB drop in magnitude), becomes an even-order polynomial in angular frequency  $\omega$ :

$$\sigma(\omega) = \sum_{n=0}^M b_{2n+1} \omega^{2n} \quad (1)$$

This even-order polynomial form of damping guarantees a causal and stable impulse response of a mechanical system [4]. For  $M = 1$ , Eq. (1) reduces to

$$\sigma(\omega) = b_1 + b_3 \omega^2 \quad (2)$$

This form of damping has been widely used in finite difference simulations, with the caution that it is only a fair approximation that matches to the experimental measurement data, and that a detailed modeling of energy loss mechanisms is absent [4].

For real-time sound synthesis of musical instruments in general, and plucked string instruments in particular, the *digital waveguide synthesis* [7, 8] provides a computationally efficient method. This method is based on the traveling wave solution of the wave equation, and the traveling waves are simulated using bidirectional digital delay lines. All the losses are consolidated into a set of discrete points, and they are simulated using low-order lowpass filters that are generally termed as loop-filters [7, 6]. A one-pole loop filter with independent gain  $g$  and frequency parameter  $a$ , i.e.

$$H_l(z) = g \frac{1+a}{1+az^{-1}} \quad (3)$$

has been a popular choice for model-based sound synthesis of plucked string instruments [6, 9].

The estimation of the loop-filter parameters is established by a method that tracks the harmonics of a recorded tone, extracts the decay characteristics of each harmonic (assuming each harmonic exhibits a pure exponential decay), converts the decay to the desired magnitude response of the loop filter, and finally obtains the filter parameters by a weighted least-squares minimization [10]. The fixed order of the filter guarantees the stability for  $|a| < 1$ . However, in each step of the estimation, some error is introduced. The total error, in turn, deviates the loop-filter parameters significantly. In order to minimize the analysis error, and compensate the measurement error, different ad-hoc approaches have been proposed [10, 11, 12].

The relation between the one-pole loop filter of Eq. (3) and the simple damping expression of Eq. (2) has been investigated in [13]. It has been shown that under certain approximations Eq. (2) can be related to the loop-filter parameters. In the same reference, two novel methods for an arbitrary-order loop filter design have been reported. The first technique in [13] minimizes the mean-square error (MSE) between the measured and desired decay times of the harmonics. This approach results in an inherently stable, arbitrary order IIR filter. The method is further elaborated in [14].

The second technique in [13] is directly based on the truncated decay rate polynomial. Assuming that the loop filter gain deviation from unity is very small, its magnitude response is approximated by a Taylor series, and thus the two-term decay rate polynomial of Eq. (2) is obtained. The formulas relating the filter coefficients to the polynomial coefficients that are obtained from measurements by regression are also given. For higher order all-pole filters, it has been assumed that the polynomial order  $M$  is equal to

the order of the filter, however this is not justified. Moreover, the optimal order of the decay-rate polynomial has been left unspecified. Once the constraint about the order is relaxed, one can obtain less and less MSE by increasing the polynomial order. However, there is a danger that the approximation matches the irregularities of the measured data instead of the desired target function.

This paper aims to present robust and reliable methods that can be used for loop filter design. It introduces the decay rate polynomial of Eq. (1) as an intermediate step, provides the background for truncating the infinite-order polynomial of Eq. (1) at an order  $\hat{M}$  that is derived from the measurement data. Once  $\hat{M}$  is found, it determines the number of damping terms to be included in the finite difference simulation. Moreover, methods are shown for designing an arbitrary order recursive loop-filter from the truncated polynomial.

The structure of the paper is as follows. In Sec. 2, an alternative formulation of the loop-filter design problem is stated and a brief overview of the statistical model-selection methods is given. Sec. 3 demonstrates the important concepts related to the problem; it shows the estimation of  $\hat{M}$ , and presents a loop-filter design method based on the  $\hat{M}$ th-order polynomial. Sec. 4 draws the conclusions.

## 2 PROBLEM FORMULATION

The problem in this paper is a *semi-parametric polynomial regression* problem, i.e., the problem of estimating the parameter vector  $\mathbf{b}$  and the order  $M$  of a function  $F(\mathbf{b}(\hat{\sigma}_k), M(\hat{\sigma}_k), \omega)$  from a set of  $K$  noisy measurements  $\hat{\sigma}_k$ . The basis functions of  $F(\cdot)$  are prescribed, and given in Eq. (1). The estimation is based on minimizing a prescribed norm, so that

$$\|\hat{\sigma}_k - F(\mathbf{b}(\hat{\sigma}_k), M(\hat{\sigma}_k), \omega)\| \approx 0 \quad (4)$$

An alternative way of formulating the problem is considering the approximation error, which is usually a result of two distinct mechanisms: model mismatch, and measurement inaccuracies [15]. Consider another set of samples, say  $\bar{\sigma}$ , that are generated by a more complex model than  $F(\cdot)$  account for, such as the physical damping mechanisms in musical strings. Then the measured set  $\hat{\sigma}$  may be regarded as  $\bar{\sigma}$  contaminated with measurement inaccuracies. Model mismatch results in an error in Eq. (4) even when the ideal and noiseless sample set  $\bar{\sigma}$  is used. Measurement inaccuracies account for the deviation of the data  $\hat{\sigma}$  from  $\bar{\sigma}$ .

In this alternative formulation, the optimum model is obtained by a joint minimization of the following subproblems:

$$\|\hat{\sigma}_k - \bar{\sigma}\| \approx 0 \quad (5a)$$

$$\|\bar{\sigma} - F(\mathbf{b}, M, \bar{\sigma}, \omega)\| \approx 0 \quad (5b)$$

Note that the least-squares techniques assume a priori that Eq. (5a) is satisfied with equality, and focus on Eq. (5b) without further considering the validity of Eq. (5a). Emerging algorithms propose alternative methods to relax this inherent assumption [15]. Also note that Eq. (5a) is a  $K$ -dimensional minimization problem, whereas Eq. (5b) has  $M$ -degrees of freedom. In other words, the joint minimization redistributes  $K$  samples onto a  $M$ -dimensional space. It can be shown that  $K^M$  samples

are needed for a model with  $M$  parameters to achieve the same sample distribution with an univariate model to be tuned with  $K$  samples [16]. Since the number of available data samples are usually fixed, higher dimensional models are more prone to introduce larger errors in Eq. (5b) compared to the lower dimensional models, although they achieve better performance minimizing the MSE in Eq. (4). In order to equalize this difference, the total error estimate is obtained by adjusting (penalizing) the MSE of Eq. (4) with a function that depends on the degrees of freedom  $M$  of a model, and the available samples  $K$ .

All known analytical model selection criteria for polynomial regression problems estimate the total error using the following expression [16]:

$$MSE_{\text{total}} \cong \phi\left(\frac{M}{K}\right) MSE \quad (6)$$

where  $\phi$  is a monotonically increasing function of the ratio of degrees of freedom  $M$  and sample size  $K$ . In effect, the penalization function  $\phi$  inflates the MSE for increasingly complex models. Some of the analytical model selection methods proposed in the statistical literature are *Final prediction error* (FPE), *Shwartz criteria* (SC), *Generalized cross-validation* (GCV), and *Shibata's model selector* [16], and their penalization functions are given by:

$$\phi_{\text{FPE}}(p) = \frac{1+p}{1-p} \quad (7a)$$

$$\phi_{\text{SC}}(p, K) = 1 + \frac{1}{2} \log(K) \frac{p}{1-p} \quad (7b)$$

$$\phi_{\text{GCV}}(p) = \frac{1}{(1-p)^2} \quad (7c)$$

$$\phi_{\text{SMS}}(p) = 1 + 2p \quad (7d)$$

where  $p = M/K$ . These methods are proven by asymptotic arguments regarding the sample size, and are known to give suboptimal (lower) model order estimates for very small number of samples. Moreover, they also assume that the estimation method is unbiased, i.e., the approximation sample set contains the target function. However, these criteria are applied in practical situations when the underlying assumptions do not strictly hold, and reported to perform well in these cases [16].

Eq. (6) provides the key for solution of the decay rate estimation problem. The measurement data of size  $K$  is fitted by truncated polynomials up to the order  $N$ , and for each order the MSE of the fit has been penalized using Eq. (6). The minimum of the total error gives the desired order. Before the demonstration of the method, however, it is instructive to consider the sources of the measurement errors.

### 2.1 The measurement error

For the present problem, the set of decay rates  $\hat{\sigma}_k$  are to be extracted from the measured string instrument tones. Although a subset of the tools that are used for loop-filter design [10, 11, 12] may be utilized for this purpose, as mentioned in Sec. 1, the additional errors introduced by these techniques are inevitable. An example about the performance of these tools are given below.

The data set consists of anechoic classical guitar tones of the first (sample groups 1 and 2), and the fourth (sample groups 3 and 4) strings, played by a professional musician by varying the finger (index, middle, and thumb),

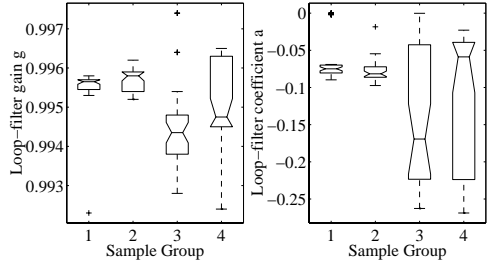


Figure 1: Distribution of the extracted one-pole loop filter parameters.

the dynamics (piano, forte, fortissimo), and the plucking style (apoyando and tirando). 18 samples of seventh fret positions (sample groups 1 or 3) and another 18 of open positions (sample groups 2 or 4) of each string have been recorded. The tones have been analyzed with the tools that are described in [12, 9], and the parameters of the one-pole loop filter (see Eq. (3)) have been extracted for each sample.

The extracted parameters are shown by sample groups in Fig. 1. A standard box plot have been used, where the tick inside each box is the median value, the box boundaries contain the 25% of the data, the ticks connected to the boxes with dashed lines contain the 75% of the data, and the crosses are outliers. The scattering of the parameters is evident in the figure. A desirable method should reduce the variance for each parameter and converge to their main values. In the following sections, such a method is introduced. In order to bypass the effects of the analysis tools and provide a better focus on the proposed method, synthetic data has been used throughout this paper.

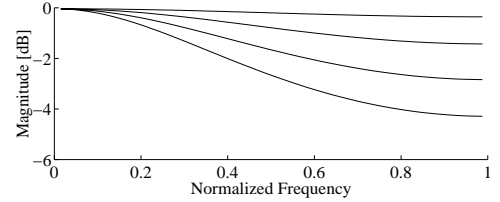
### 3 SIMULATIONS

The three simulations presented in this section are conducted to illustrate the relationship between the decay rate function and the filter magnitude response, the estimation of the optimum order  $M$  (in the sense that the truncated polynomial model jointly minimizes Eq. (5a) and Eq. (5b)), and designing a loop filter based on the truncated order polynomial, respectively. In order to avoid confusion that may occur because of the even-order nature of the polynomial model, throughout the simulations, the order will be represented by  $N = 2M$ .

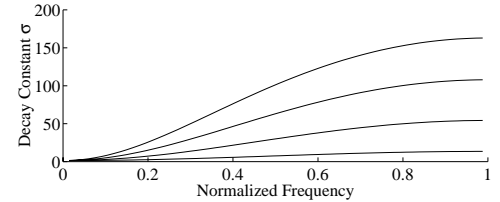
#### 3.1 Decay rates in the absence of noise

In this simulation, the mean values of the  $a$  and  $g$  parameters for the highest string ( $f_0 = 330\text{Hz}$ ) have been used as template (sample group 2 in Fig. 1). The one-pole loop filter magnitude responses have been calculated by varying the coefficient  $a_m = ma_{\text{mean}}$  where  $m = \{.5, 1, 2, 3\}$ . The gain  $g_{\text{mean}}$  has been kept fixed. The resulting four magnitude responses are shown in Fig. 2(a) for increasing  $m$  (from top to bottom). The magnitude of the filter is related to the decay times of the harmonics as follows

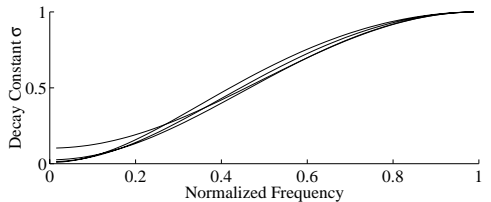
$$|H(e^{j\omega_k})| = e^{-\frac{1}{f_0} \tau_k} \quad (8)$$



(a) The magnitude responses



(b) Corresponding decay rate functions



(c) Normalized decay rate functions

Figure 2: The illustration of the relationship between the one-pole loop filter and the decay rate functions.

The decay rate functions are obtained by

$$\bar{\sigma}(\omega_k) = \frac{1}{\tau_k} = -f_0 \log(|H_m(e^{j\omega_k})|) \quad (9)$$

at 66 harmonic frequencies within the audio range. Note that  $\bar{\sigma}(\omega_k)$  correspond to the ideal sample set of Eq. (5a), and  $K = 66$ . The resulting decay rate functions are shown in Fig. 2(b). The curves follow the opposite ordering with the loop filter magnitude responses: the highest decay rate corresponds to the coefficient  $a_3$  that has the highest deviation in the magnitude response from the unity.

One may have the impression from Fig. 2(b) that the different absolute values of the target functions may weight the MSE of the polynomial regression for each case, thus no conclusions can be deduced from the comparison of the MSE corresponding to each of the target functions. In order to suppress this weight, target functions are normalized by dividing them to their maximum values, and this normalized function set shown in Fig. 2(c) is used in the simulation.

Fig. 3 plots the polynomial order versus the MSE (in dB scale) of the approximation of the normalized decay rate functions of Fig. 2(c). For each case, the approximation error decreases exponentially (linear on dB scale). With the same order of approximation, the MSE depends on the  $a$  coefficients of the generating filters. In

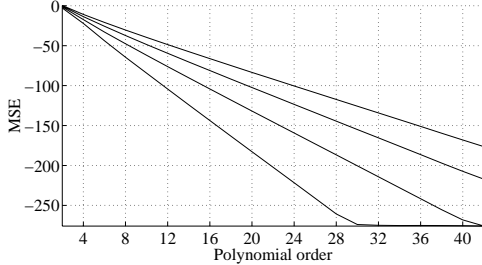


Figure 3: The MSE for increasing order polynomial approximation to the target samples  $\hat{\sigma}_m(\omega_k)$ .

$b_1$	$b_3$	$b_5$	$b_7$	$b_9$	$b_{11}$	$b_{13}$	$b_{15}$
0.167	0.112						
0.049	0.231	-0.014					
0.030	0.271	-0.027	0.001				
0.026	0.283	-0.033	0.002	0	0		
0.026	0.286	-0.036	0.003	0	0		
0.026	0.287	-0.037	0.004	0	0		
0.026	0.287	-0.037	0.004	0	0	0	
0.026	0.287	-0.038	0.004	0	0	0	0

Table 1: The increasing order polynomial parameters of the approximation to the target sample set.

other words, given a target MSE, say -100 dB, the target function  $\hat{\sigma}_{1/2}(\omega)$  should be approximated by a 12th order polynomial,  $\hat{\sigma}_1(\omega)$  by a 16th order,  $\hat{\sigma}_2(\omega)$  by a 18th order, and  $\hat{\sigma}_3(\omega)$  by a 24th order polynomial, respectively.

This example illustrates that the truncation order  $N$  cannot be directly related to the filter order, i.e., the order  $N$  of the decay rate polynomial cannot determine the filter order uniquely. Note that both the shape and the decay rate of a target function can be associated with the  $L^2$  norm of the difference between the generating filter magnitude response and unity, i.e.,  $\|1 - |H(e^{j\omega})|\|_2$ . This association may be used as an axillary smoothness criterion to establish a relation between the filter order and the decay-rate polynomial order. This remark is an elaboration of a similar conclusion stated in [13].

The convergence characteristics of the approximation can be checked from Table 1, where the polynomial coefficients are tabulated for the target sample set generated by the loop-filter  $H_1(z)$  that has the mean coefficients. The convergence regime fits the lowest order parameter first, then proceeds with higher order parameters.

Note that the convergence is not completed at  $N = 1$ , corresponding to the two-term polynomial in Eq. (2). In other words, in most practical cases the simple one-pole loop filter simulates a more complicated damping regime compared to the damping models of the form in Eq. (2).

### 3.2 Decay rates in the presence of noise

In order to consider the actual nature of the problem, Gaussian noise with a high variance has been added to the target decay rate function. The ideal target function, as well as its noisy samples are shown in Fig. 4. No attempts have been made to shape the noise according to the physical phenomena and actual measurement errors. Moreover, it has been assumed that the decay rate estimates are available within the audio range.

The polynomial regression is performed by increas-

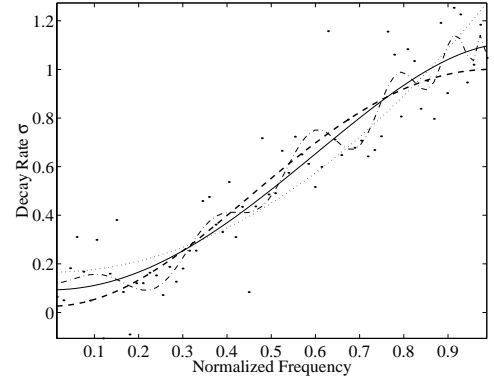


Figure 4: Approximation to the noisy sample set (dots) by the second, fourth, and twenty-fourth order polynomials, shown with dotted, solid, and dash-dotted curves, respectively. The target function is shown with a dashed curve.

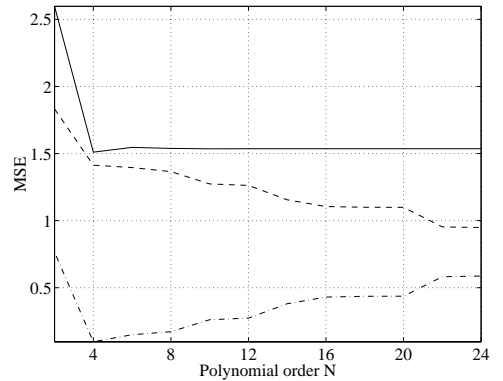


Figure 5: The empirical, actual, and total MSE of the approximation, shown by dash-dotted, dashed, and solid lines, respectively.

ing the order  $N$ . The figure shows the second, fourth, and twenty-fourth order polynomial fits with dotted, solid, and dash-dotted lines, respectively. As in the noiseless case, the second order polynomial exhibits a high deviation from the target function. The fourth order polynomial seems to exhibit similar characteristics to those of the target function, whereas the twenty-fourth order polynomial deviates again from the target function, providing rather a better fit to the noise characteristics.

It is instructive to investigate the *empirical*, *actual*, and *total* MSE, i.e., the MSE between the noisy samples and the fitted model, the MSE between the noiseless samples of the target function and fitted model, and the sum of the empirical and actual MSE. Note that the empirical MSE corresponds to the error imposed by the Eq. (4), whereas the actual MSE corresponds to the error imposed by Eq. (5b). It is clear that the empirical MSE decreases by increasing the model order, however the sample values of the higher-order polynomials deviate more and more from the actual (noiseless) values of the target function. The total error has a minimum at  $\hat{N} = 4$ . This order and the error is the correct solution of the problem by considering both the Eq. (5a) and the Eq. (5b).

Fig. 6 shows the total MSE estimates obtained from

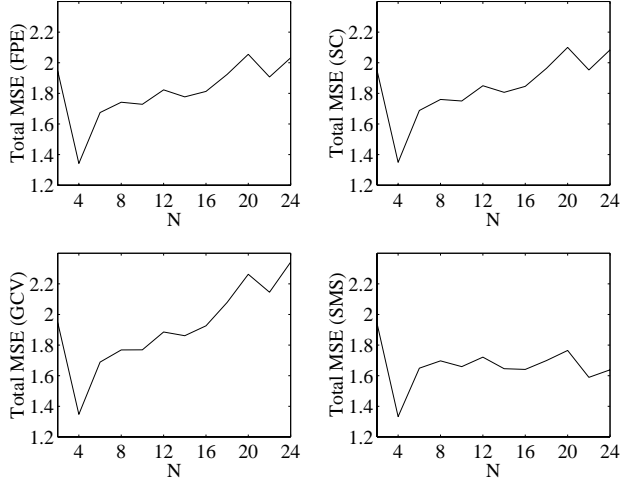


Figure 6: The estimates of the total MSE by Final Prediction Error (FPE), Shwartz criteria (SC), Generalized Cross Validation (GCV), and Shibata's model selector (SMS).

the analytical model selection criteria mentioned in Sec. 2. The estimates are calculated using Eq. (6) and corresponding penalization function  $\phi$  for each method. All the methods have a distinct global minimum at order four, which is the correct order for the particular data set used in the simulation. The total error estimates at this order are slightly lower than the total MSE in Fig. 5, but this fact is of minor importance, since in a minimization problem, the absolute value of the MSE is not needed. Moreover, the comparison of Fig. 5 and Fig. 6 shows that all the methods but SMS tend to over-penalize the higher-order polynomials. This is related to the fact that they converge into the target total MSE asymptotically, as the sample size  $K \rightarrow \infty$ . Therefore it is a good practice to obtain model-order estimates from multiple model-selection criteria and average their predictions in order to obtain reliable estimates.

### 3.3 Loop-filter design

Once the optimum  $\hat{N}$  has been found, it is straightforward to obtain the desired magnitude spectrum using the following relation:

$$|H_{\hat{N}}(e^{j\omega})| = e^{-\frac{\sigma_{\hat{N}} \omega}{f_0}} \quad (10)$$

The next task is design a filter  $H_l(z)$  minimizing  $\| |H_{\hat{N}}(e^{j\omega})| - |H_l(z)|_{z=e^{j\omega}} \|$ . This problem looks similar to the initial problem of Eq. (4) in form, however there are fundamental differences. First of all, the new problem is an approximation problem rather than a regression problem, since both terms are real, continuous functions of a single variable  $\omega$ . Moreover, there is no measurement error, i.e., the intermediate polynomial representation turns the problem of Eq. (4) into a form similar to that of Eq. (5b) only, by satisfying Eq. (5a) automatically. In this case, total MSE equals to the empirical MSE, and there is a unique least-squares solution for this problem. The problem can also be turned into a weighted least-squares problem by a weighting function. In addition, the desired magnitude response does not exceed unity, thus the designed loop filter guarantees a stable virtual string model.

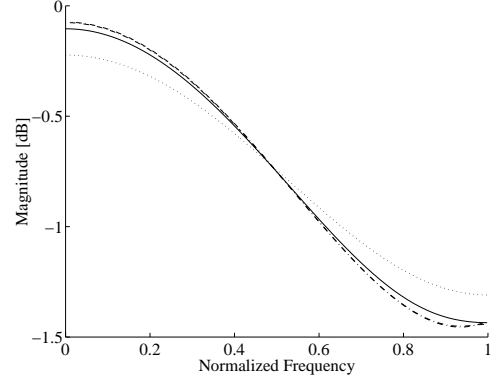


Figure 7: The desired magnitude response (dash-dotted) obtained from the truncated polynomial and the magnitude responses of the fitted IIR filters. The filter orders are one, two, and six, and they are plotted with dotted, solid, and dashed respectively.

For obtaining the loop filter coefficients, MATLAB `yulewalk` function has been used. This function is based on modified Yule-Walker algorithm for an arbitrary-order IIR filter design. Other methods, such as the one proposed in [14], may be utilized for solution as well. Fig. 7 shows the designed filter magnitude responses of the first, second, and sixth order IIR filters together with the desired magnitude response obtained from Eq. (10). The response of the 6th order IIR filter is completely overlapping with the desired magnitude response, so that this two magnitude responses can hardly be distinguished.

As a final step, it is instructive to compare the magnitude response of the filter that generated the simulation data to the response of the designed filter, both shown in Fig. 8. The dots are the noisy samples of the generating magnitude response at multiples of a test fundamental frequency  $f_0 = 330$  Hz. The magnitude response corresponding to the truncated decay rate polynomial (calculated by Eq. (10) after obtaining the order that minimizes the total MSE) is shown with a dashed curve. Finally the fitted biquad filter response is shown with a solid curve. Although there are slight deviations, the responses are very close to each other. It is evident that the effect of the noise is efficiently by-passed, hence the presented method is robust under simulation conditions. However, evaluation of the performance of the suggested method with measurement data has been left as a challenging future task.

## 4 CONCLUSIONS

In this paper the problem of designing a stable loop filter for virtual string instruments have been investigated. The simulated decay-rate samples, which can also be obtained by measurements, have been used as an intermediate design step. The distinction between the empirical and total MSE of the polynomial regression using these samples has been emphasized in a general framework. Four different methods of analytical model selection, have been used to illustrate how the obtain the optimum polynomial order, in the sense that the truncated polynomial minimizes the total MSE. A simple method for designing the final filter has been shown. The results indicate that the method is both robust and reliable.

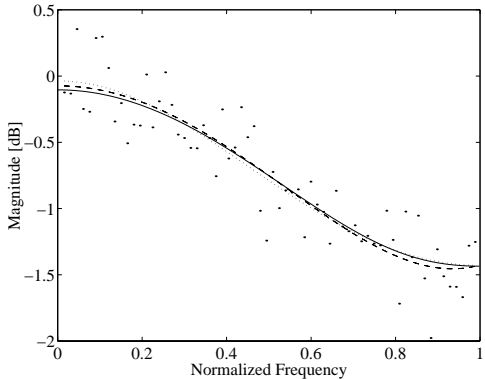


Figure 8: Comparison of the generating filter response (dotted), the magnitude response corresponding to the truncated polynomial (dashed), and fitted biquad filter magnitude response.

There are some points that need further investigation. It would be desirable to obtain another criterion that helps to determine the loop-filter order as well. Since this problem differs from the polynomial regression, the analytical methods cannot be incorporated as such. The simulation in Sec. 3.1 indicates that the relation between the filter and polynomial order is not one-to-one, however there is a relation between the smoothness of the filter magnitude response and the polynomial order. This relation needs to be quantified, and should be incorporated in the design process.

The perception of the decay-rate differences is another important topic. In fact, recent perceptual studies show that large errors in the decay characteristics of the plucked string tones may be tolerated by the listeners [17]. However, at their recent level, these studies are providing just qualitative insight rather than quantitative rules. Therefore, the method presented in this paper does not rely on perceptual criteria. Once elaborated, perceptual criteria may be incorporated in the method as well.

## 5 ACKNOWLEDGMENTS

The author wishes to thank Dr. Vesa Välimäki for fruitful discussions. This work was financed by the Academy of Finland. The work of the author has been supported by the Jenny and Antti Wihuri Foundation. The help of J. Bensoam and T. Hélie by writing and providing a L<sup>A</sup>T<sub>E</sub>Xstyle file, respectively, for the typesetting of this paper is also acknowledged.

## REFERENCES

- [1] N. H. Fletcher and T. D. Rossing, *The Physics of Musical Instruments*. New York: Springer-Verlag, 1991.
- [2] C. Valette, "The mechanics of vibrating strings," in *Mechanics of Musical Instruments* (A. Hirschberg, J. Kergomard, and G. Weinreich, eds.), pp. 116–183, Wien - New York: Springer, 1995.
- [3] A. Chaigne, "On the use of finite differences for musical synthesis. Application to plucked stringed instruments," *Journal d'Acoustique*, Vol. 5, No. 2, 1992, pp. 181–211.
- [4] A. Chaigne and A. Askenfelt, "Numerical simulations of piano strings. I. A physical model for a struck string using finite difference methods," *J. Acoust. Soc. Am.*, Vol. 95, No. 2, Feb. 1994, pp. 1112–1118.
- [5] D. A. Jaffe and J. O. Smith, "Extensions of the Karplus-Strong plucked-string algorithm," *Computer Music J.*, Vol. 7, No. 2, 1983, pp. 56–69. Also published in Roads C. (ed). 1989. *The Music Machine*, pp. 481–494. The MIT Press, Cambridge, Massachusetts, USA.
- [6] M. Karjalainen, V. Välimäki, and T. Tolonen, "Plucked-string models: From the Karplus-Strong algorithm to digital waveguides and beyond," *Computer Music J.*, Vol. 22, No. 3, 1998, pp. 17–32.
- [7] J. O. Smith, "Physical modeling using digital waveguides," *Computer Music J.*, Vol. 16, No. 4, 1992, pp. 74–91.
- [8] J. O. Smith, "Principles of digital waveguide models of musical instruments," in *Applications of Digital Signal Processing to Audio and Acoustics* (M. Kahrs and K. Brandenburg, eds.), pp. 417–466, Boston: Kluwer Academic Publishers, 1998.
- [9] M. Laurson, C. Erkut, and V. Välimäki, "Methods for modeling realistic playing in plucked-string synthesis: analysis, control and synthesis," in *Proc. of DAFX-00*, (Verona, Italy), 2000. An extended version of this paper has been accepted for publication in *Computer Music Journal*.
- [10] V. Välimäki, J. Huopaniemi, M. Karjalainen, and Z. Jánosy, "Physical modeling of plucked string instruments with application to real-time sound synthesis," *J. Audio Eng. Soc.*, Vol. 44, No. 5, May 1996, pp. 331–353.
- [11] T. Tolonen, "Model-based analysis and resynthesis of acoustic guitar tones," Master's thesis, Helsinki University of Technology, Espoo, Finland, Jan. 1998. See <http://www.acoustics.hut.fi/publications/>.
- [12] C. Erkut, V. Välimäki, M. Karjalainen, and M. Laurson, "Extraction of physical and expressive parameters for model-based sound synthesis of the classical guitar." Presented at the 108th AES Int. Convention 2000, Paris, France, preprint no. 5114, Feb. 2000.
- [13] B. Bank, "Physics-based sound synthesis of the piano," tech. rep., Helsinki University of Technology, Laboratory of Acoustics and Audio Signal Processing, 2000. See <http://www.acoustics.hut.fi/publications/>.
- [14] B. Bank and V. Välimäki, "Robust loss filter design for digital waveguide synthesis of string tones." Unpublished manuscript, submitted for publication in Dec. 2000.
- [15] A. Yeredor, "The extended least squares criterion: Minimization algorithms and applications," *IEEE Transactions on Signal Processing*, Vol. 49, No. 1, Jan. 2001, pp. 74–86.
- [16] V. Cherkassky and F. Mulier, *Learning from data: Concepts, Theory, and Methods*. John Wiley and Sons, Inc, 1998.
- [17] T. Tolonen and H. Järveläinen, "Perceptual study of decay parameters in plucked string synthesis." Presented at the 109th AES Int. Convention, Los Angeles, USA, preprint no. 5174, Sept. 2000.